ORIGINAL ARTICLE

Hydrogeophysical investigation at El Moghra Area, North Western Desert, Egypt

Sultan A. S. Araffa[1] · **Maha Abdelazeem[1]** · **Hassan S. Sabet[2]** · **Ahmed M. Al Dabour[3]**

Abstract

El Moghra area, in the western desert of Egypt, is an important part of the national reclamation project (1.5 million acres—6.07×10^9 m^2), which depends on the groundwater of El Moghra Formation (MF), the main aquifer in this area. Moghra Oasis and its surroundings are characterized by vast areas of good soil, which are favorable for agricultural development. In this respect, ambitious plans and successful programs are urgently required. Thirty-one vertical electrical sounding stations (VES's) were measured in El Moghra. The results of quantitative interpretation of such stations and well logging data indicate that the subsurface stratigraphy of the investigated area consists of six geo-electrical units where the main aquifer is represented by the fourth and sixth units intercalated with a clay unit (fifth unit). Thirteen boreholes of depth reaching 200 m are drilled in the study area. The hydrochemical analyses for collected samples indicate that the salinity of the groundwater in the Moghra area increases with depth. The result of the pumping test for boreholes indicates that the efficiency of the wells is ranging from 65 to 96% of the average value of 84.5%. The aquifer has transmissivity which represents a highly potential aquifer.

Keywords Geoelectric method · Geophysical borehole logging · Pumping test · Chemical analyses · Moghra · Aquifer

Introduction

Geophysical tools, especially the electric resistivity methods, can be used to delineate groundwater distribution. Many authors used the geophysical tools for groundwater exploration (e.g. Abdelazeem et al. 2018; Araffa et al. 2017, 2013; Al-Garni et al. 2005). Araffa et al. (2017) applied 3-D VES inversion and shallow seismic refraction techniques to delineate groundwater and subsurface structures at the northwestern part of the Gulf of Suez, Egypt. Sultan et al. (2017) evaluated the groundwater potentiality at south Ataqa, northwestern part of the Gulf of Suez, using resistivity data. Araffa et al. (2015) applied integrated geophysical interpretation to delineate the structural elements and

groundwater aquifers at the central part of the Sinai Peninsula, Egypt. Araffa (2013) delineated the groundwater aquifer and subsurface structures in north Cairo, Egypt, through the integrated interpretation of magnetic, gravity, and geoelectrical data. Sultan et al. (2009) also applied geophysical techniques at the Central Part of the Sinai Peninsula, Egypt for groundwater exploration and subsurface mapping. Gheorhge (1979) has a critical review of the processing and synthesis of hydrogeological data. However, different authors used geoelectrical methods in groundwater exploration such as Al-Garni et al. (2005) in wadi Lusab, Makkah Almukarramah, Saudi Arabia; Ariyo and Adeyemi (2009) on Fidiwo/Ajebo areas of Southwestern Nigeria; Hasan et al., 2019 on alluvial aquifers of Lower Bari Doab, Pakistan; and Bello et al. (2010) applied geostatistical analyses of accuracies of geologic sections derived from interpreted vertical electrical soundings (VES) data. Akhter and Hasan (2016) applied geoelectrical sounding and pumping test data for the determination of aquifer parameters in Khanewal District, Pakistan. De Lima et al. (2015) used a volumetric approach for the resistivity response of freshwater shaly sandstones. Singh et al. (2019) delineated the fracture zone for groundwater using a combined inversion technique in the premises

✉ Sultan A. S. Araffa
  sultan-awad@yahoo.com

1   National Research Institute of Astronomy and Geophysics, NRIAG, Helwan, Cairo, Egypt

2   Geology Department, Faculty of Science, Al-Azhar University, Cairo, Egypt

3   The General Company for Research and Groundwater and Green Valley for Logging, Cairo, Egypt

of Central Institute of Mining and Fuel Research (CIMFR), Dhanbad, Jharkhand, India. Maréchal et al. (2004) used hydraulic tests at different scales to characterize fracture network properties in the weathered-fractured layer of a hard rock aquifer in Maheshwaram, 30 km from Hyderabad (Andhra Pradesh, India).

The Egyptian government is now very interested to investigate groundwater aquifers for reclamation. El Moghra area is representing an important part of the Egyptian 1.5 million feddan (acres 6.07×10^9 m^2) national reclamation project. The area of study has been subject to numerous geological and hydrogeological studies (Abdelazeem et al. 2020, 2019; Khan et al. 2014). Khalifa (2014) studied sustainable groundwater management in El-Moghra aquifer and concluded that the decreases of groundwater exploitation will definitely lead to the sustainable development of the study area as a result of the decreases of the drawdown in El-Moghra aquifer. Mohamaden et al. (2016) applied the electrical resistivity method for groundwater exploration at the Moghra area, Western Desert, Egypt and concludes that the study area is composed of four geoelectrical units of different resistivity values. Omara and Sanad (1975) studied the rock stratigraphy and structural feature of the area between Wadi El Natrun and the Moghra Depression (Western Desert), Egypt. Pickford et al. (2009) suggested the presence of Palaeoforest in the Moghra region at the time of deposition. El-Sayed and Morsy (2018) concluded that Moghra is an unconfined aquifer, composed of sands, siltstone, and calcareous shale. The groundwater flow is mainly from NE directions towards Al Qattara Depression westwards. Rizk and Davis (1991) indicated that the Miocene Moghra aquifer directly underlies the Qattara Depression, extending to the east and dipping beneath younger formations to the north. The Qattara Depression is a sink for ground-water flow from the Nile Delta aquifer in the east, the Mediterranean Sea in the north, and the Nubian artesian aquifer in the south. They concluded, through modeling, that the formation of the reservoir could cause a 30-m rise of the Moghra aquifer's water table in the central part of the Qattara Depression. This rise in the water table decreases to the north and east. Transient simulations indicate that steady-state conditions in the modeled area of the Moghra aquifer are not likely to be reached during the expected 100-year lifetime of the reservoir. The groundwater moves mainly from NE to the SW, i.e. towards Al Qattara Depression acting as a natural discharge area. The average hydraulic gradient is about 0.0005 (El Sayed and Morsy 2018). However, the previous studies were predominantly based on surface data. Contrarily, the current study is based on surface and subsurface data, which were collected from recent boreholes and geophysical data. The integration of geoelectric and well logging data can give reasonable results and a clear picture of the subsurface water-bearing formations. El Moghra Oasis and its vicinities are located in the northeast part of Qattara mega delta in north Western Desert of Egypt, about 40 km south of El Alamein (Fig. 1a). It extends between latitudes 30°00′–30°25′ N and longitudes 28°20′–29°20′E. The main target of the present study is delineating the saturated sandstone units, determining the salinity of groundwater (TDS), and the efficiency of groundwater aquifer.

Geologic setting

Stratigraphically, Moghra Lake and its vicinities are covered by different rock units ranging in age from Lower Miocene to Recent. The stratigraphic succession can be subdivided into the following rock units from base to top (Fig. 1b). The Lower Miocene deposits in the area under study can be represented by Moghra Formation (Said 1962) and are composed of fluvio-marine sediments which grades northwards to more marine facies called Mamura Formation. The fauna of Moghra Formation reveals that these deposits accumulated in swamps and lakes in which forests were present (Pickford et al. 2009). Moghra Formation is the main aquifer in the area under study, where it can be subdivided into three members from base to top as El Raml, Bait Owian, and Monquar El Dowi members according to Omara and Sanad (1975). El Raml unit is almost deposited in a fluvial environment while Monquar El Dowi unit is formed in a fluvio-marine environment. The Middle Miocene deposits are represented by the Marmarica Formation which is composed mainly of marine fossiliferous carbonates. Marmarrica Formation covers almost the northern stretch of the Western Desert. The Pliocene rock unit is called El Hagif Formation (Late Pliocene) and is composed mainly of smoky white unfossiliferous limestone with marl interbeds. It is recorded in the northeast of Moghra Oasis. It is composed of whitish limestone with shale and evaporite layers (Omara and Sanad 1975). The Quaternary sediments are represented by sand sheets, sand dunes, and sabkha. Sabkha is a coastal, supratidal mudflat or sandflat in which evaporite-saline minerals accumulate as the result of semiarid to arid climate. A sand sheet covers vast areas in Moghra Oasis and is composed mostly of fine to coarse sand; Sand dunes occupied the southern part of the oasis that takes NW–SE direction. They are the northern part of Ghard Abu El Mahariq and composed mostly of fine to medium sand. Sabkha deposits are recorded around Moghra Lake and the northwestern part of Moghra Oasis (around petroleum road).
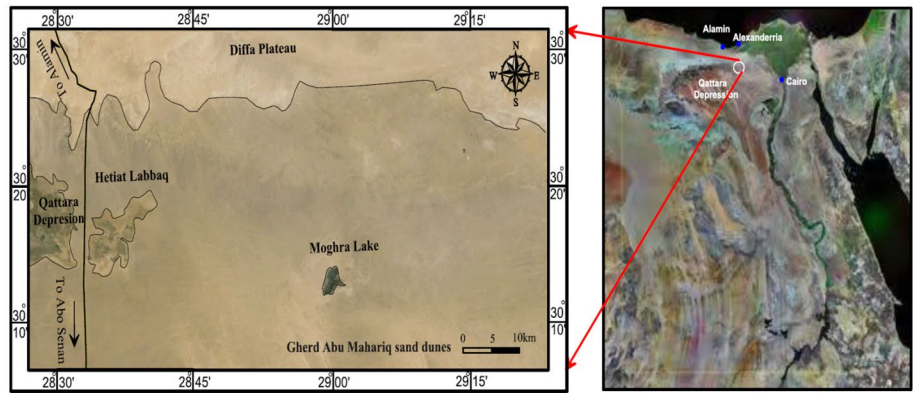
Methodology

Geoelectric data

Geoelectric data acquisition and interpretation

The geoelectrical data, used in this study, consists of 31 vertical electrical soundings (VES's). The method is based
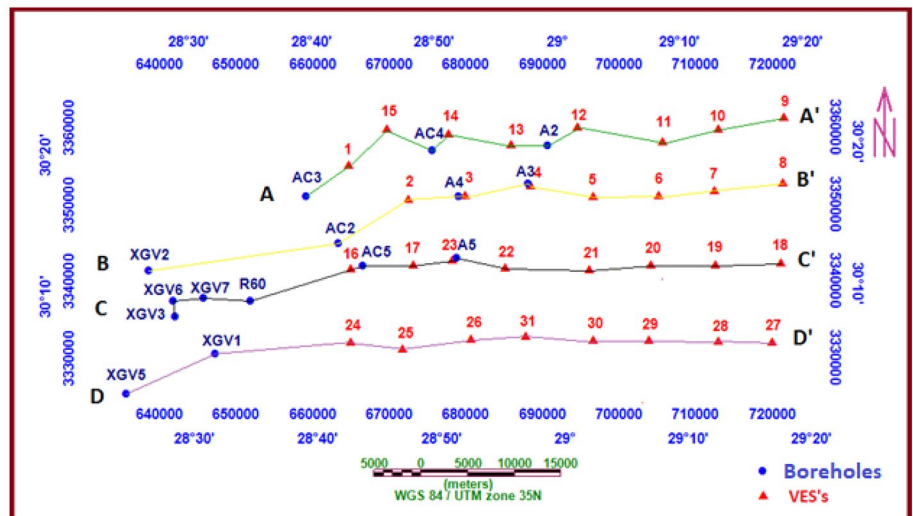
Fig. 1 **a** Location of the study area. **b** Geological map of Moghra Oasis and its vicinities, modified after Conoco (1987). **c** Location map of the boreholes and VES

(a)　Location of the study area
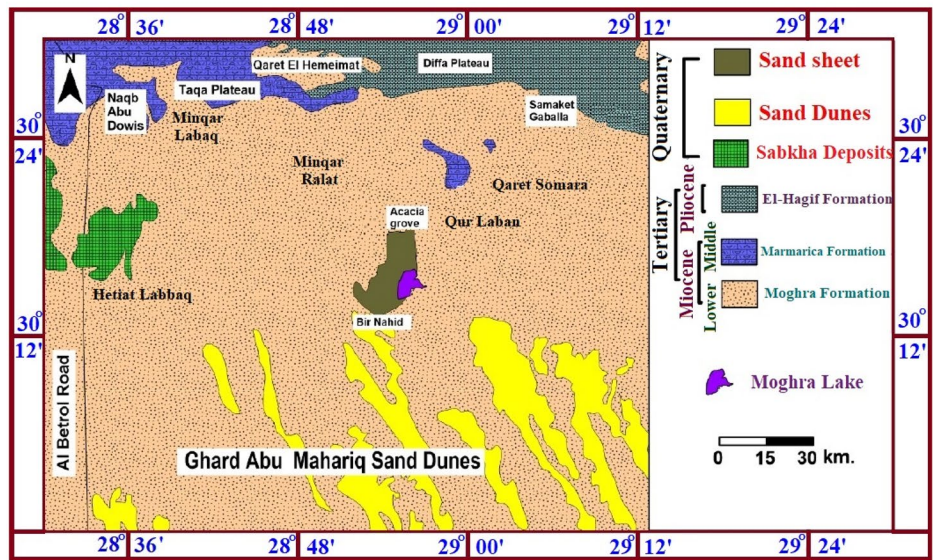
(b)　Geological map of Moghra Oasis and its vicinities, modified after CONOCO 1987.

(c)　Location map of the boreholes and VES.

on the estimation of the electrical conductivity or resistivity of the medium. The estimation is performed based on the measurement of voltage of the electric field induced by the distant grounded electrodes (current electrodes). VES measurements are carried out using the Schlumberger configuration with AB/2 (AB represents the distance between current electrodes) spacing ranges from 1 to 500 m using Syscal-R2 instrument made by IRIS Company, France. The main objective is to investigate the Moghra aquifer in the study area (Fig. 1c).

The quantitative interpretation of geoelectrical data is carried out through two techniques, the first technique is the manual interpretation using two layers master curves and the generalized Cagniard graphs, Koefoed (1960). The results of manual interpretation are used as initial model parameters for the second technique which is known as the analytical technique. The authors used IPI2WIN software (Bobachev et al. 2008) for the analytical technique to compute the inverted depths and resistivities for each VES curve. To verify the geoelectrical interpretation results, one VES station (VES 3) is measured beside borehole number A4. The borehole data are used as constraints for our subsurface model. Figure 2 shows borehole A4 logging data, which reveals that El Moghra aquifer is associated with a sandstone layer at depth −48 m from sea level representing the main aquifer in the El Moghra area. The results of the quantitative interpretation of VES's data are used to construct four geoelectrical cross sections. (Fig. 3a and b).

The comparison of VES, well logging data (Natural Gamma-ray), and drilling cutting samples are used to construct geologic cross-sections. The gamma-ray log measures the total natural gamma radiation emanating from a formation. Different types of rocks emit different amounts and different spectra of natural gamma radiation. In particular, clay usually emits more gamma rays than other sedimentary rocks, such as sandstone, gypsum, salt, coal, dolomite, or limestone because of the presence of radioactive potassium as a common component in their clay content and because the cation exchange capacity of clay causes them to adsorb uranium and thorium. This difference in radioactivity between clay and sandstone rocks allows the gamma-ray tool to distinguish between clay (high gamma-ray) and non-clay (low gamma-ray). The geoelectrical cross sections reveal six main geoelectrical units; the first unit is composed of gravel and sand of high resistivity values ranging from 102 to 2445 Ω.m and thickness of few meters. The second geoelectrical unit is characterized by varying resistivity values ranging from 19 to 1868 Ω.m and consists of sandstone intercalated with clay. The third one is composed of clay with low resistivity values ranging from 0.1 to 9 Ω.m. The fourth unit consists of sandstone and exhibits moderately to high resistivity values ranging from 21.7 to 1358 Ω.m, which represents the top of El Moghra aquifer. The fifth

geoelectrical unit is composed of clay which reveals low resistivity values ranging from 0.7 to 8.8 Ω.m. The sixth geoelectrical layer represents the main aquifer in the area under study where all boreholes, penetrated and produce groundwater for agriculture from this unit and exhibits moderately to low resistivity values ranging from 43.7 to 97.2 Ω.m. The previously recorded layers are dissected by eleven normal faults (F1–F11) that affected the lithologic continuity of these layers.

Static water level

The interpretation of VES stations was also used to estimate the static water level for El Moghra aquifer. Topographic map of the El Moghra study area showing absolute elevation of up to 155 m above sea level in the northern and southeastern parts of the study area. In the center and to the northwestern parts, a depression is located with a depth of −42 m below sea level. The wells are indicated as red dots, the VES location as black triangles. (Fig. 4a), also, the depth to water level increases from −5 m at the western part to −185 m at the eastern part of the area as shown in (Fig. 4b).

Borehole data

Thirteen boreholes are drilled in the western part of the study area (Fig. 5a), according to the results of VES interpretation, with depths reach to 200 m, to delineate the configuration of Moghra aquifer, evaluate the hydraulic parameters, and investigate the subsurface lithology.

Geologic cross sections

The well logging data and core samples are used to construct three geologic cross-sections along three profiles as shown in (Fig. 5a). The geologic cross-sections indicate that the subsurface section is composed of five geologic layers, the first layer represents the surface layer, which is composed of sand, sandstone, gravel, and clay of a few meters thickness. The second layer is formed of sandstone with clay intercalation of thickness ranging from 20 to 70 m. The third geologic layer is composed of clay, which is located at different depths with varying thicknesses. The fourth geologic layer consists of dry sandstone. The fifth layer represents the main aquifer in the study area (Moghra aquifer) which consists of sandstone intercalated with clay of undetected thickness. The geologic sections refer that the water level at −42 m below sea level as shown in (Fig. 5 b, c, and d).

Hydrochemical data

The hydrochemical data represented by pH, electrical conductivity (EC), and total dissolved solids (TDS), measured
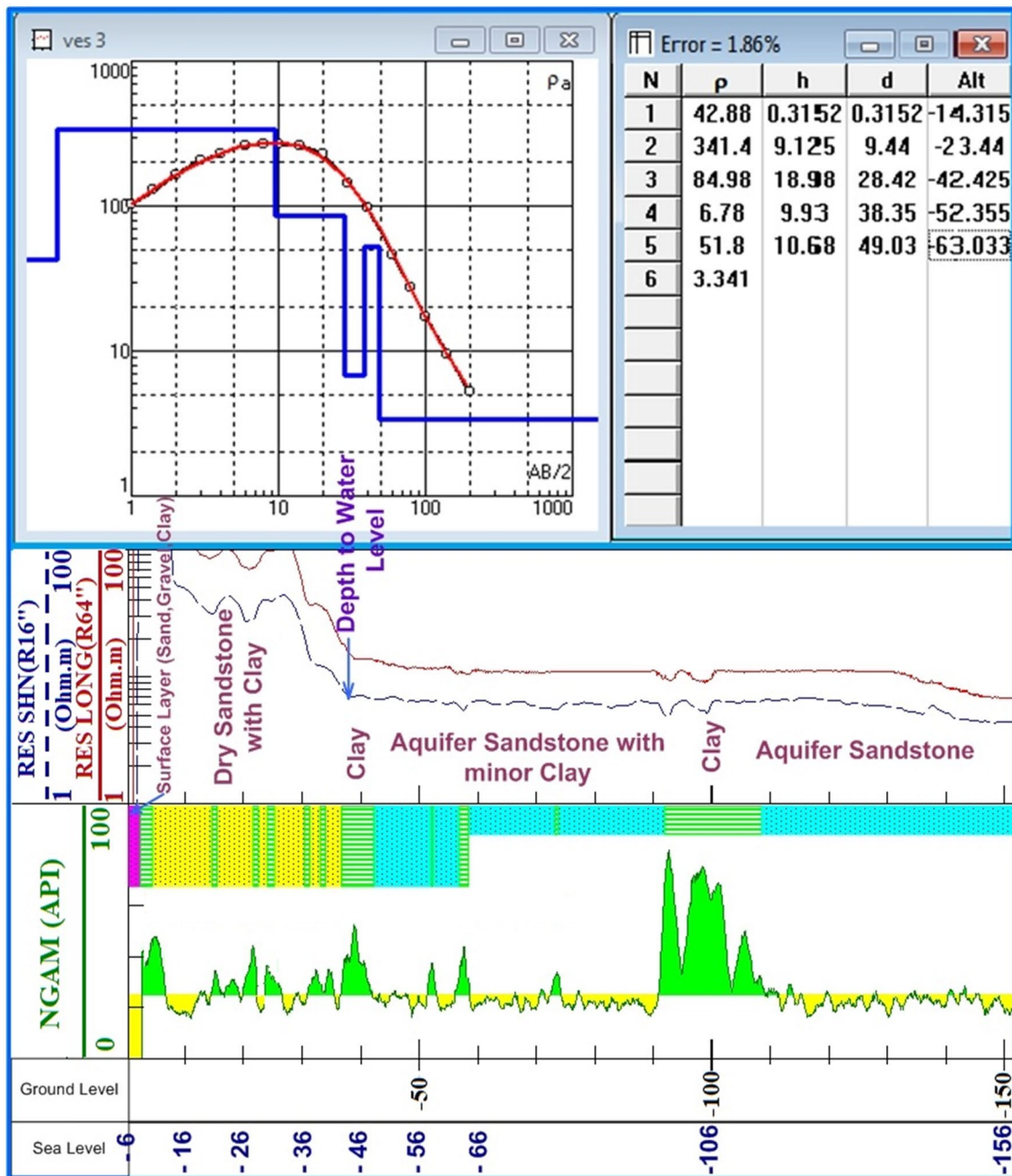
Fig. 2 Correlation between VES No. 3 indicating resistivities, thickness, depths, elevations of different units complained with Well A4.This figure indicating confirmation for water depth and rock units for both VES and borehole

at 33groundwater samples collected from El Moghra aquifer (Fig. 6a). These wells were drilled to different depths varying from 100 to 200 m. Firstly, the pH limit in the drinking and irrigation water ranges between 6.5 and 8.5 in pure water as per (WHO 1984; FAO 1985), from the results of the groundwater samples in the area of study, the pH value ranges from 6.71 to 8.70 (Fig. 6b).

Second, the electrical conductivity (EC) which means the ability of an aqueous solution to carry an electric current.

It is directly related to the total dissolved salts (ions) in the water. The obtained values of EC in the groundwater samples range from 3420 (µmhos/cm) for well no. Mo-26 to 11,800 (µmhos/cm) for well no. R-140. The distribution of EC in groundwater samples (Fig. 6c) indicates that the minimum values of EC are located at the eastern and southeastern parts while it increases toward the northwestern, southwestern, and northern parts. The conductivity is low in the east and southeastern direction due to the probable

Fig. 3 a Geoelectric cross sections along profiles A–A$^\backslash$ and B–B$^\backslash$, showing different geologic units, fault elements, borehole logs. **b** Geoelectric cross sections along profiles C–C$^\backslash$ and D–D$^\backslash$, showing different geologic units, fault elements, borehole logs
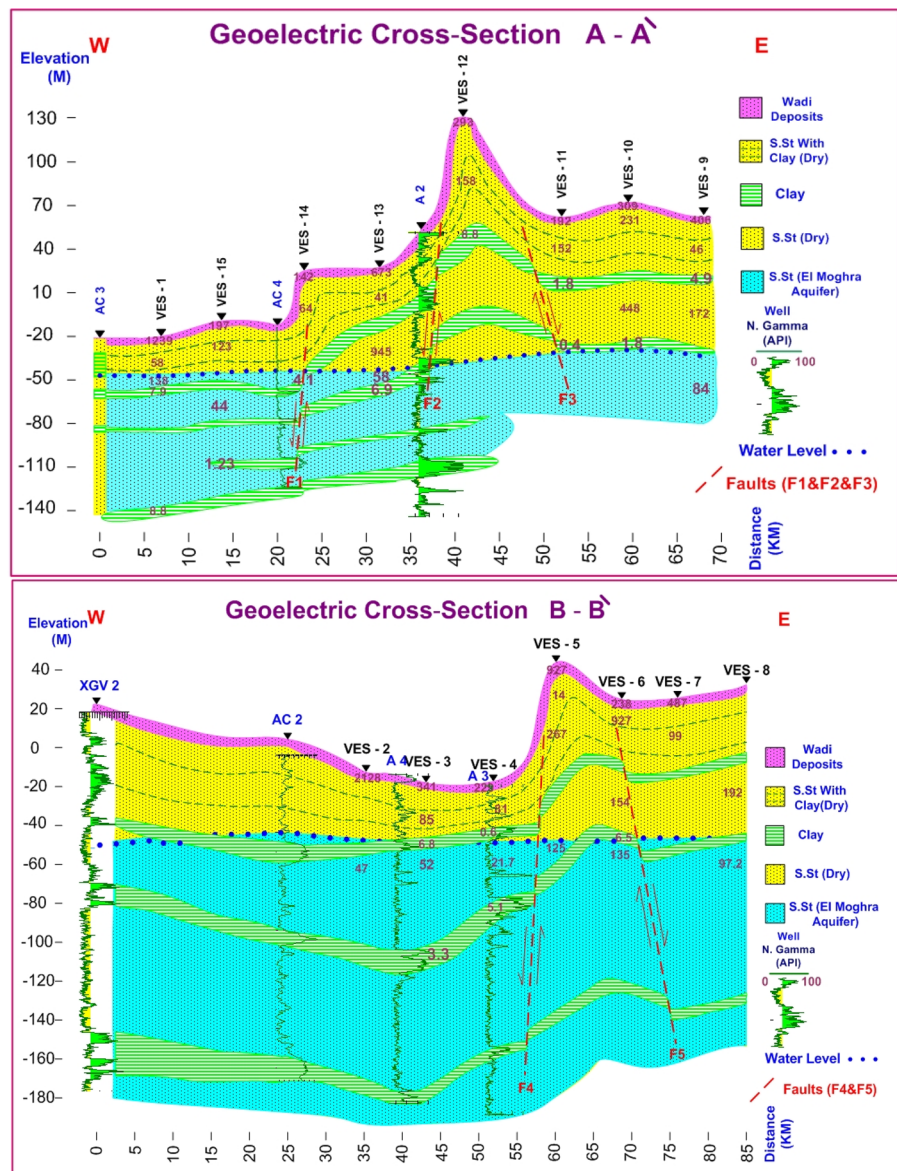
(a) Geoelectric cross sections along profiles A – A$^\backslash$ and B – B$^\backslash$, showing different geologic units, fault elements, borehole logs.

groundwater recharge from the Quaternary aquifer and due to the seepage of Wadi El Natroun groundwater through subsurface channels.

Finally, the obtained TDS in groundwater varies from 2236 (mg/l) at sample number Mo-26 to 7830 (mg/l) at sample number R-140 and there is a strong similar relationship between TDS and EC in terms of increasing and decreasing tendencies (Fig. 6d). This relationship is explained by the cross plot (Fig. 6e) which shows that the proportional relationship between TDS and EC with confidence value is 0.9 ($r^2 = 0.981$). The salinity of the groundwater in the El Moghra area increases with the depth, The Data Log for Well XGV 3 shows the resistivity (R16″ and R64″) decrease

with the depth that indicates the increase of water salinity as shown in (Fig. 6f).

Hydraulic parameters of El Moghra aquifer

The pumping tests are used to estimate the hydraulic properties and aquifer characteristics of the aquifer. The pumping test depends on measuring the discharge of the well and the resulting drawdown at a specific time. These measurements can be used to calculate the hydraulic characteristics of the aquifer. For example, the pumping test data for well R61 in the study area are step drawdown tests, constant discharge tests, and recovery tests. (Fig. 7 a, b, and c).

Fig. 3 (continued)
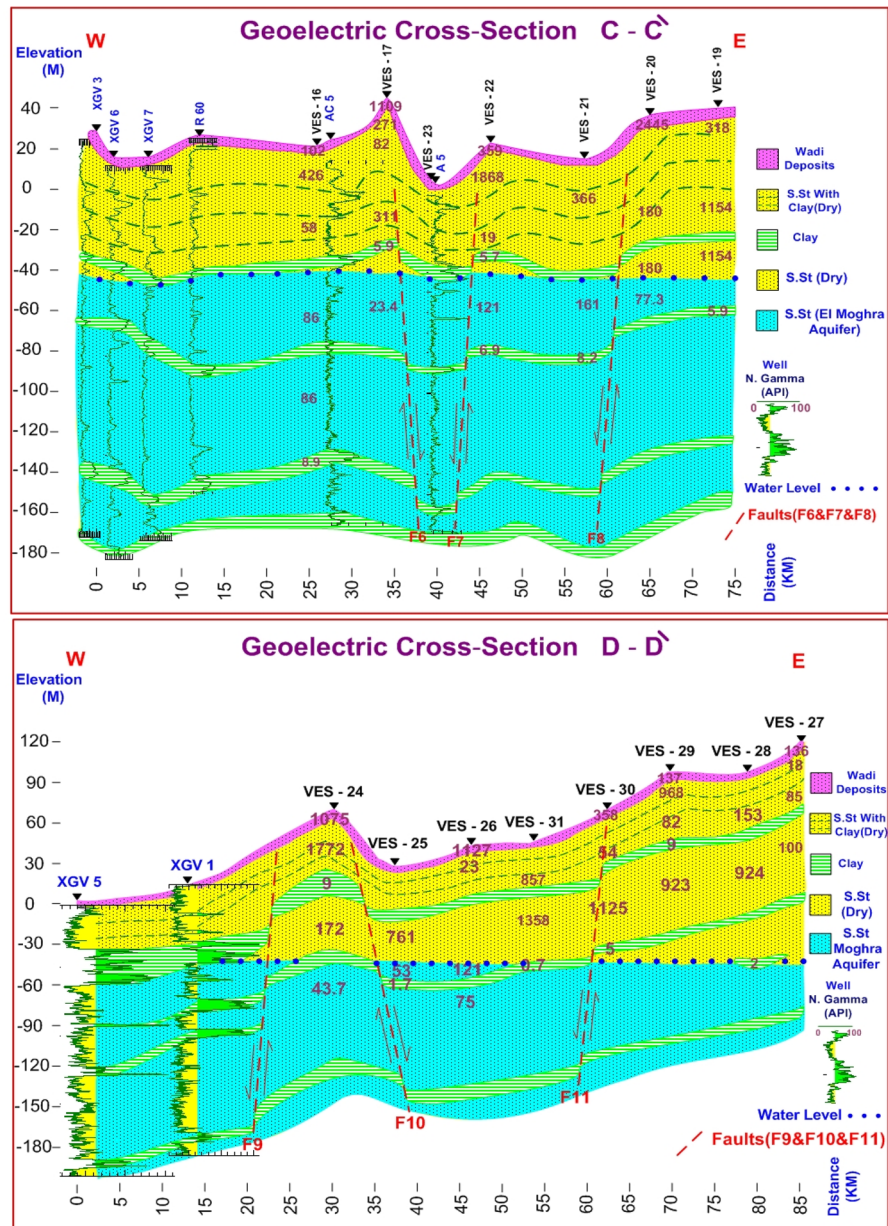
(b) Geoelectric cross sections along profiles C – C$^\backslash$ and D – D$^\backslash$, showing different geologic units, fault elements, borehole logs.

Step drawdown tests The step-drawdown test for well R61 (Fig. 7a; Table 1) is one of the most useful assessment tools for groundwater aquifer. It is a pumping test in which the drawdown in a well is observed while the discharge rate from the well is increased in steps. In a step-drawdown test, the discharge rate in the pumping well is increased from an initially low constant rate through a sequence of pumping intervals (steps) of progressively higher constant rates. Each step is typically of equal duration, lasting from approximately 30 min to 2 h (Kruseman and de Ridder 1994).

By plotting S/Q versus Q Fig. (7a) and fitting a straight line 1964through the points, the well loss coefficient C is given by

the slope of the line, and the formation loss coefficient B is given by the intercept of the line with S/Q axis (Q=0), (Todd, 1980). The total drawdown may be represented approximately by the following equation (Jacob 1964):

$$S = BQ + CQ^2, \tag{1}$$

where S is the total drawdown in m, Q is the rate of discharge in m^3/d, C is the well loss in d^2/m^5, and B is the formation loss constant in d/m^2. Thus, from the graph the formation loss $B = 2.6 \times 10^{-3}$ d/m^2 and the well loss $C = 1.8 \times 10^{-7}$
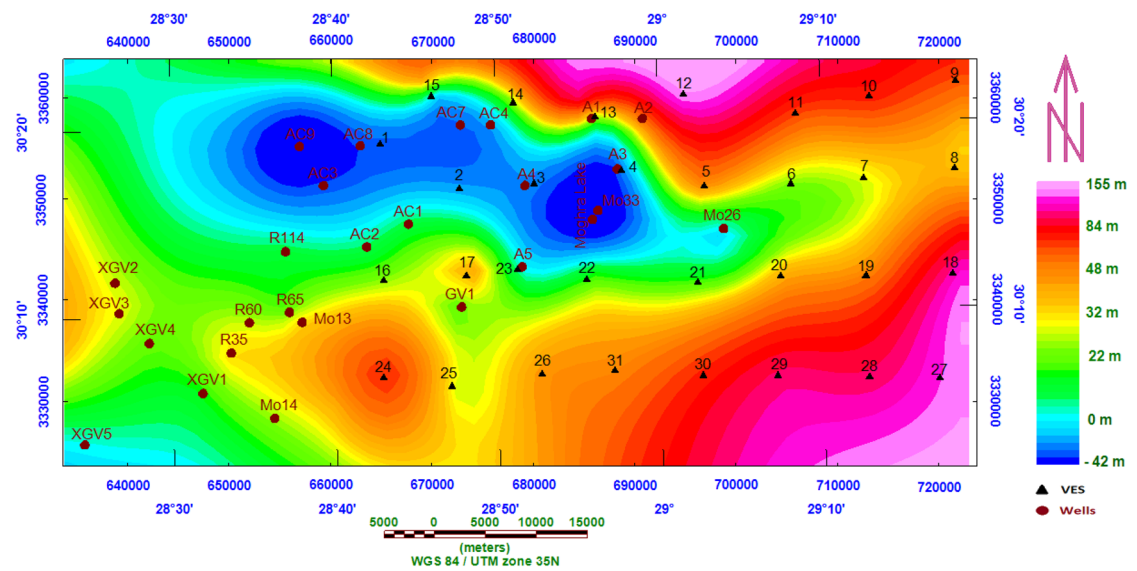
(a)   Topographic Map of the Study Area.
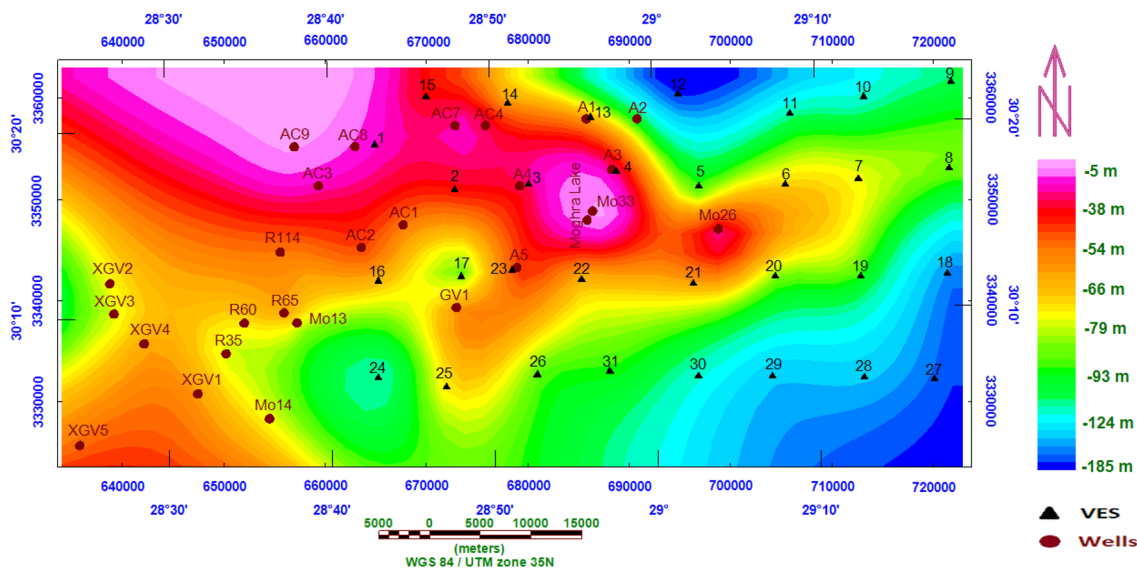
(b)   Static Water Level from Ground Surface.

Fig. 4   **a** Topographic map of the study area. **b** Static water level from ground surface

d^2/m^5. Then, we can determine well efficiency from this equation.

$$\text{Well efficiency} = (BQ/(BQ + CQ^2)) \times 100 \qquad (2)$$

The efficiency of a pumping well expresses the ratio of aquifer loss (theoretical drawdown) to total (measured) drawdown in the well. (Kruseman and de Ridder 1990). A well efficiency of 70% or more is usually considered acceptable. The average well efficiency for well R 61 in the area under study is 83.12% as shown in Table 2.

Constant discharge test and recovery test In the constant discharge test for well R61 (Fig. 7b) by plotting the observed drawdown (s) versus time (t) on a semi-logarithmic paper (t in the log scale), a straight line of slope s is obtained (Jacob 1964).

$$T = 0.183 \times Q/s, \qquad (3)$$

where, T = transmissivity (m^2/d), s = slope of line (meters/log cycle), Q = discharge (m^3/d), T_p = 1455 (m^2/d), which represents high potential aquifer (Fig. 7b). T_r = 1476 m^2/d (Fig. 7c).

T_p and T_r are transmissivity values of constant test and recovery tests. Table 3 represents the classification of the aquifer potentiality according to transmissivity values (after Gheorhg 1979).

From Table 4, the recommended safe yield of the wells (discharge Q) (m^3/h) range from 90 (m^3/h) to 160 (m^3/h) and the maximum drawdown (s) (m) range from 1.6 m

Fig. 5 **a** Locations of boreholes and geologic sections for profiles 1, 2 and 3. **b** Geologic section along profile −1 showing different geological units, fault elements, well logging records, and water level. **c** and **d** Geologic section along profile −2 and profile −3, respectively, showing different geological units, fault elements, well-logging records, and water level
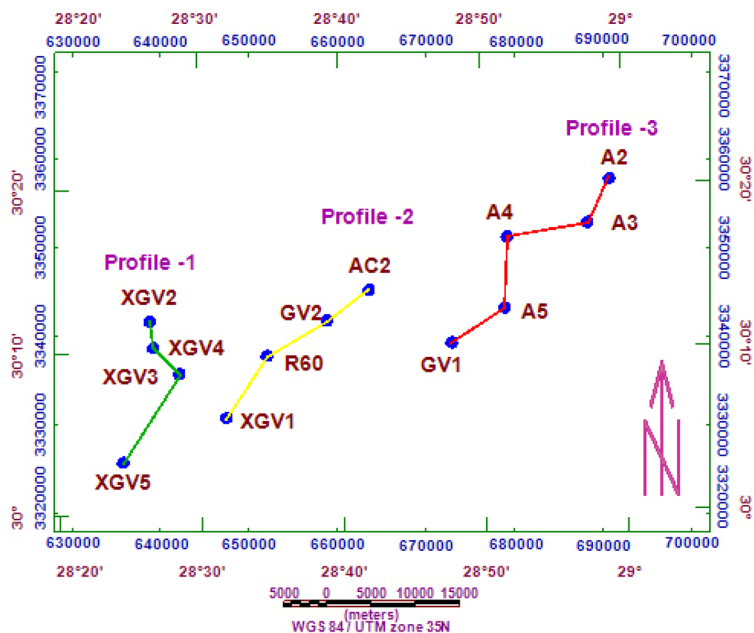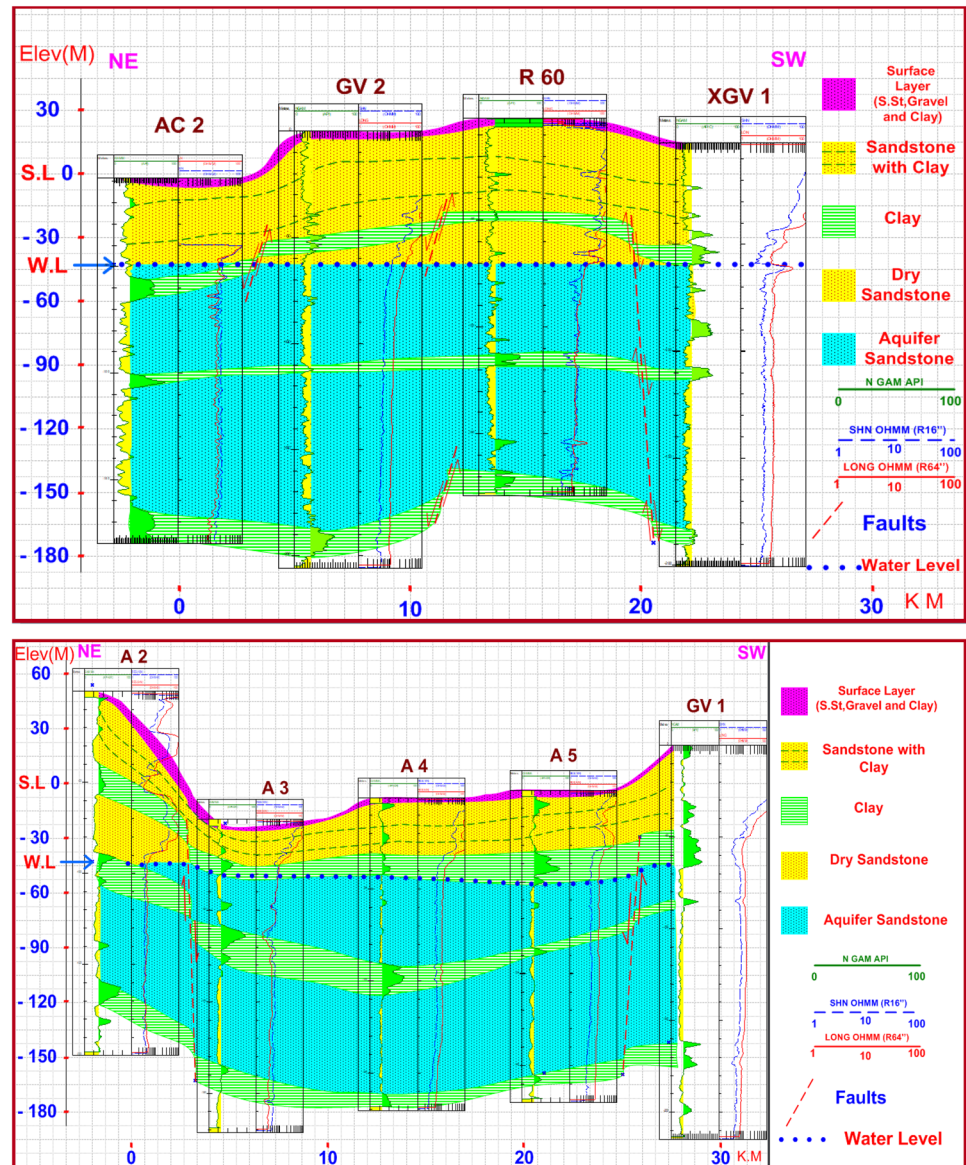

(a)   Locations of boreholes and geologic sections for profiles 1, 2 and 3
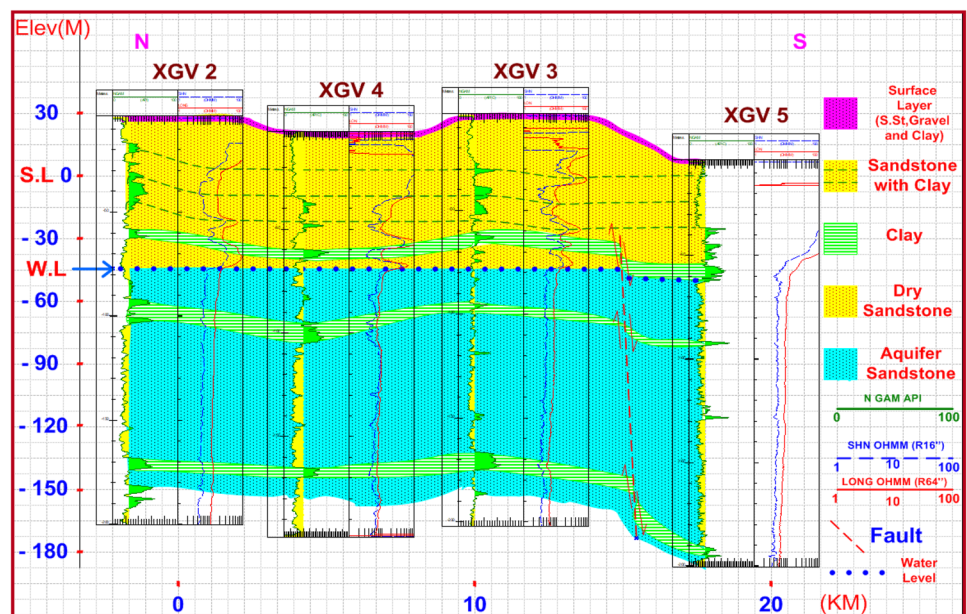
(b)   Geologic section along profile -1 showing different geological units, fault elements, well logging records, and water level.

Fig. 5 (continued)

c and d: Geologic section along profile -2 and profile -3 respectively, showing different geological units, fault elements, well-logging records, and water level.

to 12.8 m also the transmissivity for constant test (T_p) (m²/d) is ranging from 905 (m²/d) to 2895 (m²/d), while the Transmissivity for recovery test (T_r) (m²/d) is ranging from 1098 (m²/d) to 3031 (m²/d). The average of efficiency to the tested wells is 84.5%.

Discussion

The quantitative interpretation of geoelectrical data for 31VES stations, measured using AB/2 ranging from 1 to 500 m, indicates that the subsurface stratigraphy consists of five geoelectrical units, where the deeper one represents the main aquifer in the study area, which is composed of sand intercalated with clay. Thirteen boreholes were used to indicate the lithostratigraphic section, water-bearing zones' hydrochemistry, water quality, and well efficiency. The water samples from boreholes indicate that the salinity increases with depth, where the salinity increase from the east to the west of the area ranging from 2236 to 7830 PPM. Also, the electric conductivity is similar to water salinity increase from east to west and ranging from 3500 to 12,000 µmhos/cm (Fig. 6c and d). There is a linear relation between electric conductivity and water salinity in ppm as in Fig. 6e. The average well efficiency for one of the boreholes which drilled in the study area such as well R 61 is 83.12% as shown in Table 2. The Transmissivity of the aquifer according to the pumping

test for some borehole for constant test (T_p) (m^2/d) is ranging from 905 (m^2/d) to 2895 (m^2/d), while the transmissivity for recovery test (T_r) (m^2/d) is ranging from 1098 (m^2/d) to 3031 (m^2/d). The results of interpretation for resistivity data are conformable with the results of with results of boreholes data where the depth of groundwater from VES no.3 data is 38.4 m and the depth of water at borehole A4 which drilled beside VES 3 is 40 m. Also,

the depth of groundwater at VES4 is 35.4 m is a coincidence with the depth of groundwater at borehole no.A3 is 35 m. The salinity (TDS) of groundwater is increasing by depth according to hydrochemistry of samples from drilled boreholes; this increase in salinity (TDS) is compatible with results of resistivity data which refers to a decrease in resistivity values. From well-logging, data clay layer usually emits more gamma rays than other sedimentary

Fig. 6 **a** Sample location map. **b** pH contour map. **c** Electric conductivity (EC) contour map. **d** Total dissolved solids (TDS) contour map. **e** Cross plot showing the TDS and EC relationship which indicate linear relationship. **f** Total dissolved solids for Well XGV 3, this figure indicates a record of Gamma log of green color and resistivity log of black and brown color and refers to water level and salinity increase with depth
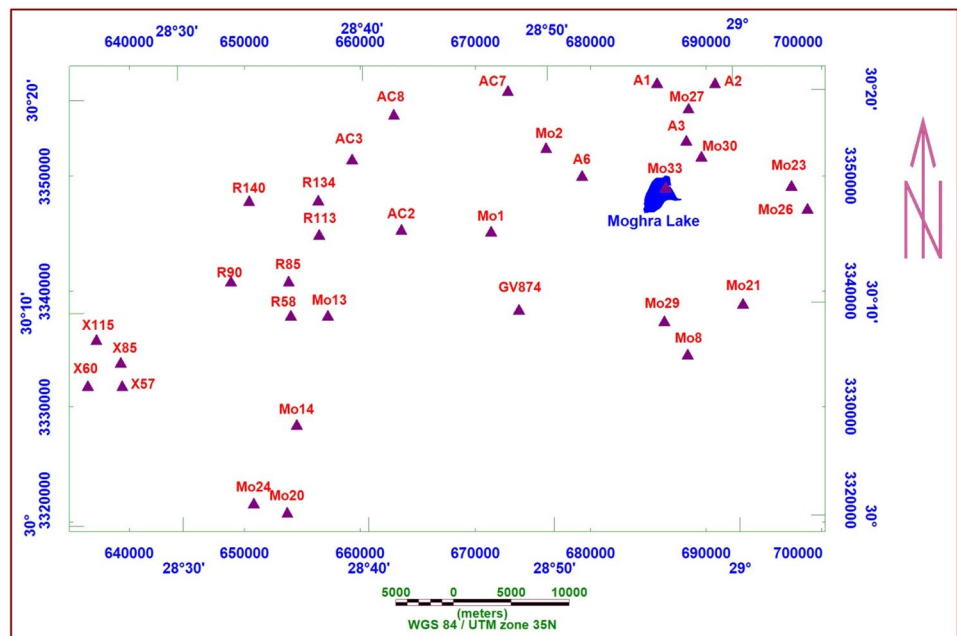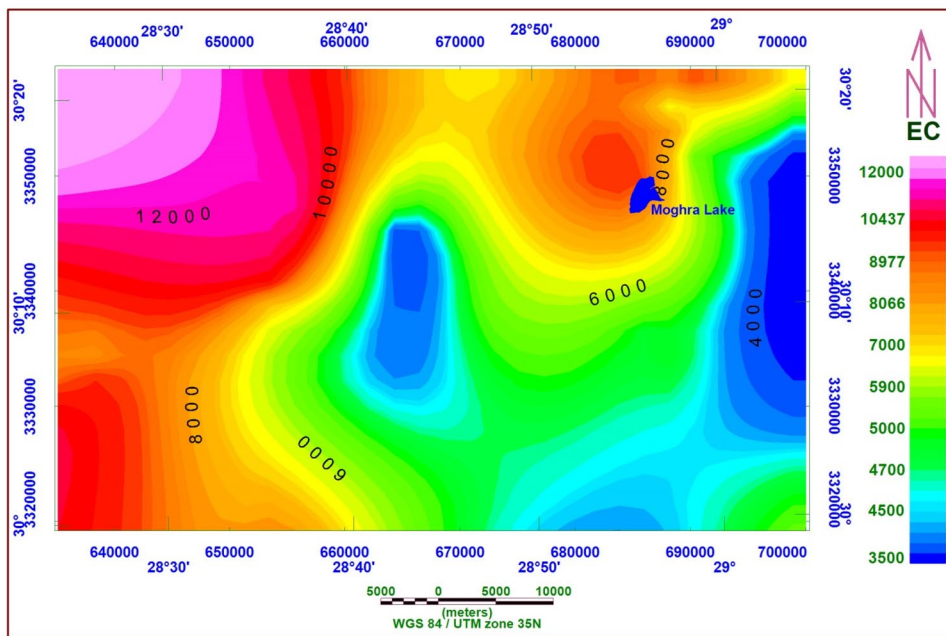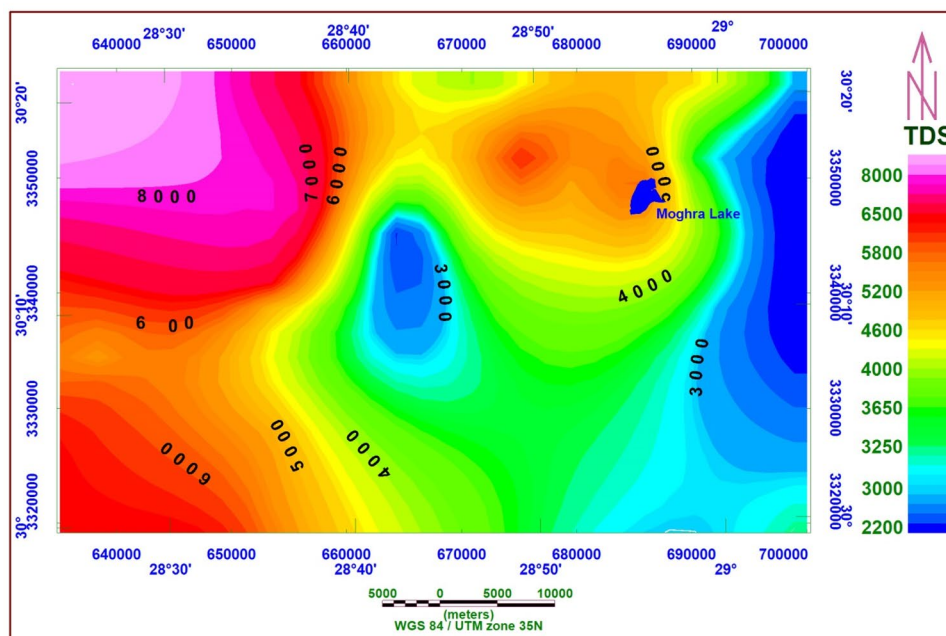

(a)　Samples Location Map
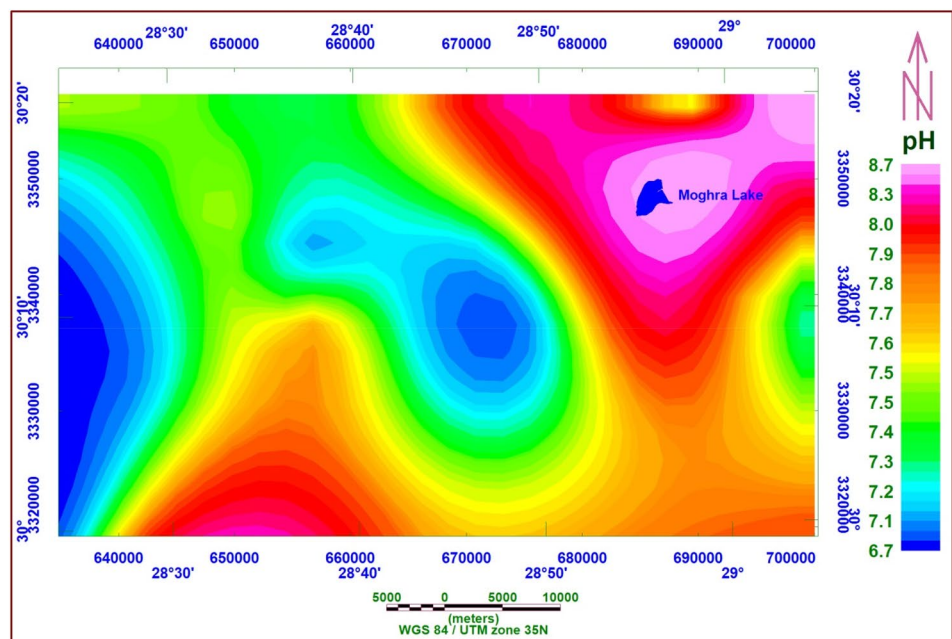
(b)　pH Contour Map

Fig. 6 (continued)


(c)   Electric Conductivity (EC) Contour Map

(c)   Total Dissolved Solids (TDS) Contour Map

rocks, such as sandstone, gypsum, salt, coal, dolomite, or limestone because radioactive potassium is a common component in their clay content and because the cation exchange capacity of clay causes them to adsorb uranium and thorium, for this reason, the Gamma-rays from well logging can be differentiated between clay layer and water-saturated sandstone where they both exhibit low resistivity values.

The results of geoelectrical data are calibrated to the results of boreholes data, which were used to constraint the resulted model, where the subsurface section consists of different units of sand and clay intercalation. The results of resistivity interpretation indicate that the aquifer is extended for more depth, as confirmed by boreholes which are drilled to a depth of 200 m where the aquifer still continuous.

Fig. 6 (continued)
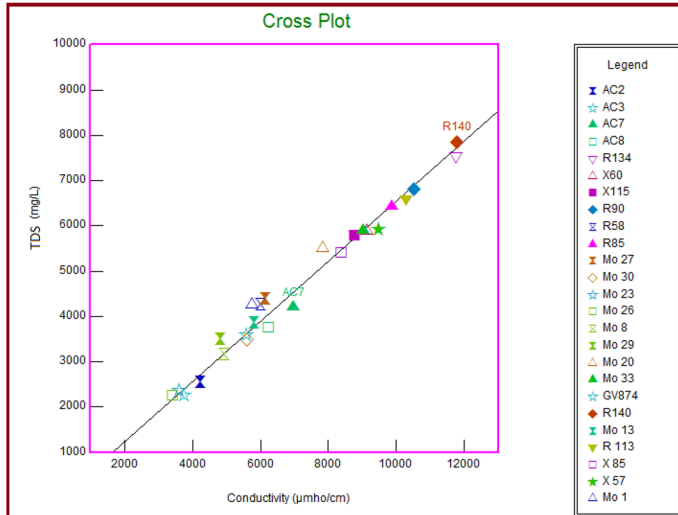
(d) Cross Plot Showing the TDS and EC Relationship which indicate linear relationship
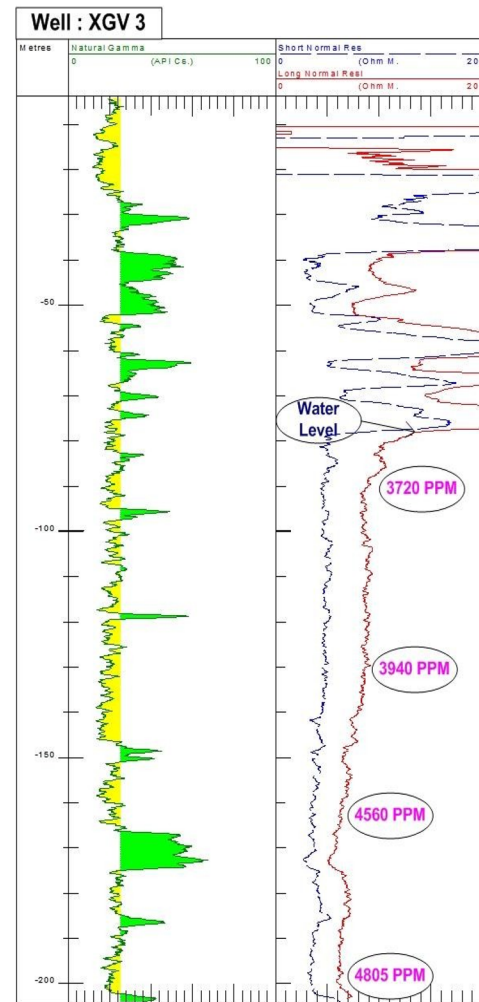

(f) Total Dissolved Solids for Well XGV 3, this figure indicates a record of Gamma log of green color and resistivity log of black and brown color and refers to water level and salinity increase with depth

The results of this work indicate that the surface layer is composed of silty clay which is suitable for agricultural purposes, where it is rich with different elements that can increase soil fertility; and the groundwater aquifer has sufficient water of different salinity values. The boreholes' depth was planned to reach 350 m, but our study results suggest reducing the depth to only 200 m. Moreover, the first plan of the project expects that the water quality increases with depth; however, the results, on the contrary, prove that the water quality decreases with depth because of salinity increase. The authors recommend using water distillation to improve the water quality by reducing the salinity of water to cultivate different types of crops.

Conclusion

The results of geoelectrical data and boreholes indicate that the study area comprises a subsurface section consisting of five geologic layers; the deepest layer represents the main aquifer in the study area (Moghra aquifer) that consists of sandstone intercalated with clay. The water level is at −42 m below sea level. The TDS value varies from 2236 mg/l (Brackish water) to 7830 mg/l (saline water). Brackish water is mainly found to be associated with the eastern part of the study area, close to Wadi El Natroun. It is suggested that the aquifer is recharged by the infiltration from the irrigation network. The groundwater salinity

Fig. 7 **a** Step-drawdown pumping test, for well R 61.this figure, represents the step test for the relation between drawdown/discharge (S/Q) on the vertical axis and discharge(Q) on the horizontal axis where the total drawdown (S) in meters can be calculated from equation $S = BQ + CQ2$, where B and C are constant can be calculated from the graph, C is the slope of the line and B is the intercept of the line with S/Q axis (vertical axis). The well efficiency from equation. Well efficiency $= (BQ/(BQ + CQ^2)) * 100$ which equal in the test to 83.12%. **b** Constant pumping test, for well R 61.this figure, this figure represents a constant test for the relation between discharge (Q) on the vertical axis and time (t) on the horizontal axis where the transmissivity (T_p) can be calculated from equation $T_p = 0.183 * Q/ s$, where the s is the slope of line then the T_p is equal 1455 (m^2/d). **c** Recovery pumping test, for well R 61, represents the recovery test for the relation between residual drawdown and t/t' where the t and t' are the time of start and end time of recovery test where the transmissivity $(T_r) = 1476$ (m^2/d)
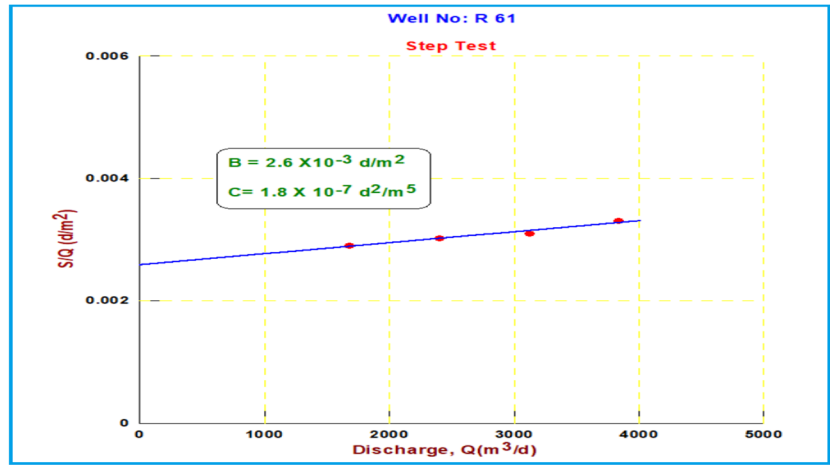
(a)
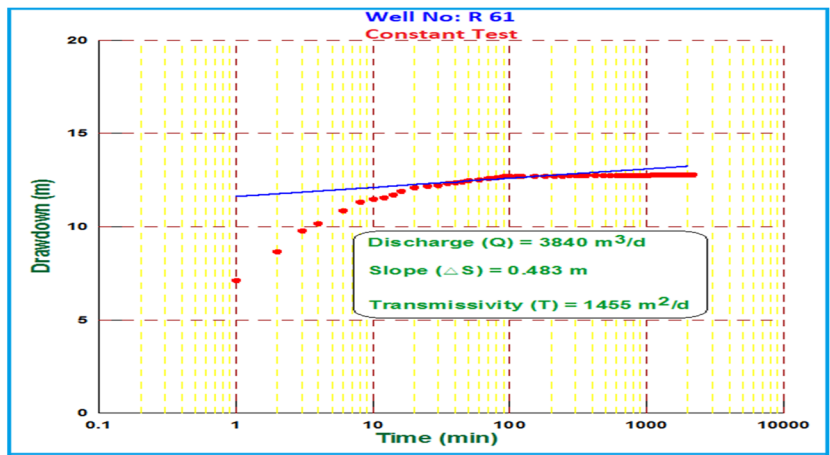
(b)
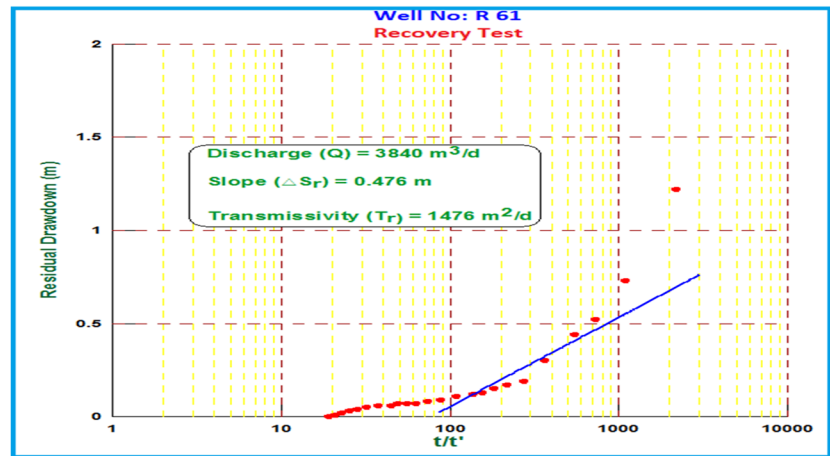
(c)

Table 1 Step drawdown test results for well R61

Step no	Discharge (Q)m³/h	Discharge (Q)m³/d	Drawdown (s) meters	s/Q (d/m²)
1	70	1680	4.88	0.0029048
2	100	2400	7.25	0.0030208
3	130	3120	9.67	0.0030994
4	160	4840	12.71	0.0033099

Table 2 Well efficiency results for well R61

Step no	Discharge (Q) m³/d	BQ	CQ²	Efficiency %
1	1680	4.37	0.51	89.58
2	2400	6.24	1.04	85.75
3	3120	8.11	1.75	82.24
4	4840	12.58	4.22	74.90
Average				83.12

Table 3 Classification of the aquifer potentiality according to transmissivity values (after Gheorhge 1979)

Potentiality of the aquifer	Transmissivity (m²/day)
Highly potential	> 500
Moderate potential	500–50
Low potential	50–5
Very low potential	5–0.5
Negligible potential	< 0.5

increases to the west and northwestern direction. The resistivity at (R16″ and R64″) decreases with depth that indicates the increase of water salinity, which is assured by the chemical analysis of wells that drilled up to 120 m have a maximum salinity of 2236 mg/l, while the salinity at wells, drilled to a depth of 200 m, reaches 7830 mg/l. The groundwater is slightly alkaline with pH value ranged from 6.71 to 8.7. The investigated area can be used for the cultivation of salt-tolerant crops (Jojoba and Olives) especially the western part of the study area. The results of the pumping test for boreholes indicate that the well efficiency ranges from 65 to 96% and the average value is 84.5%. The aquifer has transmissivity representing a highly potential aquifer. The recommended safe yield of the wells (discharge Q) (m³/h) ranges from 90 (m³/h) to 160 (m³/h) and the maximum drawdown (s) (m) ranges from 1.6 m to 12.8 m.

Table 4 Results of pumping test in ten wells in the study area

Well no results	R61	R113	AC2	AC9	AC10	AC100	GV1	XG1	XG183	XG194
Total well depth (m)	173	124	167	106	124	101	200	198	200	200
Water table (m)	71	54.22	42	5	25	32	60.32	59.8	77.8	74.1
Formation loss (B) (d/m²)	2.6×10^{-3}	8.7×10^{-4}	2.3×10^{-3}	3.4×10^{-3}	1.3×10^{-3}	1.03×10^{-3}	5.3×10^{-3}	1.3×10^{-3}	9.5×10^{-4}	1.3×10^{-3}
Well loss (C)(d²/m⁵)	1.8×10^{-7}	3.35×10^{-8}	4.4×10^{-8}	1.01×10^{-7}	6.7×10^{-8}	8.4×10^{-8}	1.01×10^{-8}	4.03×10^{-7}	2.9×10^{-7}	2.96×10^{-7}
Efficiency (%)	83	86	83	92	92.5	89.5	96	65	73	85
Discharge (Q) (m³/h)	160	100	135	127	100	100	120	100	100	90
Max drawdown (s) (m)	12.8	2.41	8.5	9.63	3.51	2.95	1.6	5.5	4.25	3.86
Transmissivity (T_p) (m²/d)	1455	2728	1976	2425	1978	2142	2895	1930	1469	905
Transmissivity (T_r) (m²/d)	1476	1910	2237	3031	2142	2440	2928	1882	1098	1432

References

Abdelazeem M, Salem ZE, Fathy MS (2020) Impact of Lithofacies and Structures on the Hydrogeochemistry of the Lower Miocene Aquifer at Moghra Oasis. Natural Resources Res, North Western Desert, Egypt. https://doi.org/10.1007/s11053-020-09679-3

Abdelazeem M, Araffa S, Salem Z, Fathy M, Saleh M (2019) Integrated Studies to Elucidate the Subsurface Structures and Groundwater at Moghra Oasis, Northwestern Desert, Egypt. In: Sundararajan N, Eshagh M, Saibi H, Meghraoui M, Al-Garni M, Giroux B. (eds.) On significant applications of geophysical methods. Advances in science, technology & innovation (IEREK Interdisciplinary Series for Sustainable Development). Springer, Cham https://doi.org/10.1007/978-3-030-01656-2_28

Abdelazeem M, Fathy M, Salem Z, Khalifa M (2018) Hydrogeochemical and geophysical studies on the shallow groundwater aquifer ay new Galala city, northern Galala plateau (Egypt). Proceeding of 1st Conference of Arabian J Geosci CAGJ, Tunisia, Hammamat, 12–15 Nov 2018

Akhter G, Hasan M (2016) Determination of aquifer parameters using geoelectrical sounding and pumping test data in Khanewal District, Pakistan. Open Geosci 8:630–638

Al-Garni MA, Hassanein HI, Gobashy MM (2005) Ground-magnetic survey and Schlumberger sounding for identifying the subsurface geologic factors controlling the groundwater flow along wadi Lusab, Makkah Al-Mukarramah, KSA. J Petrophys Geophys National Research Institute, Vol 4, 2, Cairo, Egypt

Araffa SAS (2013) Delineation of groundwater aquifer and subsurface structures on north Cairo Egypt, using integrated interpretation of magnetic, gravity and geoelectrical data. Int J Geophys 192(1):94–112

Araffa SAS, Mohamed AME, Santos F (2017) 3-D VES Inversion and shallow seismic refraction techniques for Delineating groundwater and subsurface structures using at the Northwestern part of the Gulf of Suez Egypt. Egyptian J Petroleum 26(2):457–475

Araffa SAS, El Shayeb HM, Abu-Hashish MF, Hassan NM (2015) Integrated geophysical interpretation for delineating the structural elements and groundwater aquifers at central part of Sinai Peninsula Egypt. Arabian J Geosci. https://doi.org/10.1007/s12517-015-1824-5,8:7993-8007

Ariyo SO, Adeyemi GO (2009) Role of Electrical Resistivity Method for Groundwater Exploration in Hard Rock Areas: A case Study from Fidiwo/Ajebo Areas of Southwesten Nigeria. Pacific J Sci Technol 10(1):483–486

Bello AMA, Makinde V, Coker JO (2010) Geostatistical Analyses of Accuracies of Geologic Sections derived from Interpreted Vertical Electrical Soundings (VES) Data: An Examination Based on VES and Borehole Data Collected from the Northern Part of Kwara State, Nigeria

Bobachev A, Modin I, Shevnin V (2008) IPI2Win software. A genetic algorithm approach for selecting Tikhonov regularization parameter Geoscan-M Ltd. Moscow State University. Russia. IEEE Congress on Evolutionary Computation (CEC 1–6 June 2008), https://doi.org/10.1109/CEC.2008.4631339; https://doi.org/10.1109/CEC.2008. 4631339#blank, pp. 3980–3983

Conoco (1987) Geological map of Egypt, scale 1:500,000

El-Sayed SA, Morsy SM (2018) Hydrogeological Assessment of Moghra Aquifer, North Western Desert, Egypt, Annals Geol. Surv. Egypt. V. XXXV, pp. 110 – 130

FAO (Food and Agriculture Organization) (1985) The State of Food and Agriculture. World review: the ten years since the World Food Conference Urbanization, agriculture and food systems. ISBN 92-5-102227-5 ISSN 0081-4539, 185p

Gheorhge A (1979) Processing and synthesis of hydrogeological data. Abacus, Aess, p 390

Hasan M, Shang Y, Akhter G, Jin W (2019) Application of VES and ERT for delineation of fresh-saline interface in alluvial aquifers of Lower Bari Doab. Pakistan 164:200–213

Jacob CE (1964) Drawdown test to determine effective radius of artesian well. Proc. Am. Soc. Civil Engrs. Vol. 79, No. 5

Khalifa EA (2014) Sustainable groundwater management in El-Moghra aquifer. Int J Eng Res Technol ISSN 0974–3154 Volume 7, Number 2, pp. 131–144

Khan SD, Fathy MS, Abdelazeem M (2014) Remote sensing and geophysical investigations of Moghra Lake in the Qattara Depression Western Desert, Egypt. Geomorphology 207:10–22

Koefoed O (1960) A generalized Cagniard graph for interpretation of geoelectric sounding data. Geophys Prospect 8(3):459–469

Kruseman GP, de Ridder NA (1990) Analysis and Evaluation of Pumping Test Data Second Edition (Completely Revised) ILRI publication 47. Intern. Inst. for Land Reclamation and Improvements, Wageningen, Netherlands, p 377

Kruseman GP, de Ridder NA (1994) Analysis and evaluation of pumping test data (2nd ed.), publication 47, Intern. Inst. for Land Reclamation and Improvement, Wageningen, The Netherlands, 370p

De Lima OAL, Clennell MB, Nery GG, Niwas S (2015) A volumetric approach for the resistivity response of freshwater shaly sandstones. Geophysics 70:1–10

Maréchal JC, Dewandel B, Subrahmanyam K (2004) Use of hydraulic tests at different scales to characterize fracture network properties in the weathered-fractured layer of a hard rock aquifer. Water Resources Res Am Geophysical Union 40:W11508

Mohamaden MII, Hamouda AZ, Mansour S (2016) Application of electrical resistivity method for groundwater exploration at the Moghra area Western Desert, Egypt. Egyptian J Aquatic Res 42:261–268

Omara S, Sanad S (1975) Rock stratigraphy and structural feature of the area between Wadi El Natrun and the Moghra Depression (Western Desert). Egypt Geologisches Jahrbuch 16:45–73

Pickford M, Miller ER, El-Barkooky AN (2009) Suidae and Sanitheriidae from Wadi Moghra, Early Miocene Egypt. Acta Palaeontologica Polonica 55:1–11

Rizk ZS, Davis AD (1991) Impact of the proposed Qattara Reservoir on the Moghra aquifer of northwestern Egypt. Groundwater 29(2):232–238

Said R (1962) The Geology of Egypt. Elsevier, Amsterdam, p 377

Singh KKK, Bharti AK, Pal SK, Prakash A, Saurabh Rajwardhan Kumar R, Singh PR (2019) Delineation of fracture zone for groundwater using combined inversion technique. Environm Earth Sci 78:110

Sultan AS, Essa KhSAT, Khalil MH, El-Nahry AEK, Galal AN (2017) 2017: Evaluation of groundwater potentiality survey in south Ataqa-northwestern part of Gulf of Suez by using resistivity data and site-selection modeling. NRIAG J Astronomy Geophys 6(1):230–243

Sultan SA, Mekhemer HM, Santos Fernando M, Abd Alla MA (2009) Geophysical measurements for subsurface mapping and groundwater exploration at the central part of the sinai peninsula Egypt. Arabian J Sci Eng 34(1):103–119

Todd DK (1980) Groundwater Hydrology, 2nd edn. Wiley, New York

WHO (World Health Organization) (1984) International Standards for Drinking Water. 3rd Guidelines for Drinking Water Quality. Vol. 2: Health criteria and other supporting information. Geneva, World Health Organization